

Ca²⁺ Regulates Reactive Oxygen Species Production and pH during Mechanosensing in *Arabidopsis* Roots

Gabriele B. Monshausen,^{a,b,1} Tatiana N. Bibikova,^{c,2} Manfred H. Weisenseel,^b and Simon Gilroy^a

^a Department of Botany, University of Wisconsin, Madison, Wisconsin 53706

^b Botanisches Institut, Universität Karlsruhe, 76128 Karlsruhe, Germany

^c Biology Department, Pennsylvania State University, University Park, Pennsylvania 16802

Mechanical stimulation of plants triggers a cytoplasmic Ca²⁺ increase that is thought to link the touch stimulus to appropriate growth responses. We found that in roots of *Arabidopsis thaliana*, external and endogenously generated mechanical forces consistently trigger rapid and transient increases in cytosolic Ca²⁺ and that the signatures of these Ca²⁺ transients are stimulus specific. Mechanical stimulation likewise elicited an apoplastic alkalization and cytoplasmic acidification as well as apoplastic reactive oxygen species (ROS) production. These responses showed the same kinetics as mechanically induced Ca²⁺ transients and could be elicited in the absence of a mechanical stimulus by artificially increasing Ca²⁺ concentrations. Both pH changes and ROS production were inhibited by pretreatment with a Ca²⁺ channel blocker, which also inhibited mechanically induced elevations in cytosolic Ca²⁺. In trichoblasts of the *Arabidopsis root hair defective2* mutant, which lacks a functional NADPH oxidase RBOH C, touch stimulation still triggered pH changes but not the local increase in ROS production seen in wild-type plants. Thus, mechanical stimulation likely elicits Ca²⁺-dependent activation of RBOH C, resulting in ROS production to the cell wall. This ROS production appears to be coordinated with intra- and extracellular pH changes through the same mechanically induced cytosolic Ca²⁺ transient.

INTRODUCTION

Plants are exquisitely sensitive to mechanical stimuli. Growth can be entrained to sustained mechanical loading, such as in the formation of reaction wood, and mechanically stimulated plants are often shorter and more robust (Mitchell, 1996; Braam, 2005; Meng et al., 2006). Directional mechanical stimuli can also be converted to coordinated growth responses, such as thigmotropism (e.g., Jaffe et al., 2002). At a molecular level, mechanostimulation has been characterized to elicit events ranging from rapid and widespread transcriptional changes (e.g., Braam and Davis, 1990; Kimbrough et al., 2004; Walley et al., 2007; Leblanc-Fournier et al., 2008) to ethylene and jasmonate production (Mitchell, 1996; Tretner et al., 2008).

However, mechanical stresses are not only imposed by the environment but are also generated endogenously as an inevitable consequence of the expansive growth of pressurized cells. For highly polarized cells, such as root hairs and pollen tubes, control of expansion-related mechanical stresses seems to be a fundamental aspect of growth regulation (Dutta and Robinson, 2004; Monshausen et al., 2007, 2008a). At the tissue and organ

level, mechanical forces may even drive cellular patterning (Hamant et al., 2008).

While the molecular basis for perception of a mechanical stimulus remains to be identified, the widespread demonstration of rapid increases in cytosolic Ca²⁺ in response to touch has led to models of plant mechanosensing via Ca²⁺ channels in the plasma membrane, analogous to mechanically gated Ca²⁺ channels reported for mammalian cells (reviewed in Liedtke, 2008; Monshausen et al., 2008b; Monshausen and Gilroy, 2009).


Ca²⁺-dependent proteins, such as those encoded by the TCH genes, have been proposed as downstream elements closely linked to the initial Ca²⁺ signal in this touch response system (e.g., Braam et al., 1997). Similarly, the complex and genome-wide alterations in gene expression patterns seen to accompany mechanostimulation in aerial and root tissues (Kimbrough et al., 2004; Lee et al., 2005) likely represent responses to signals such as the Ca²⁺ changes generated by initial mechanoperception. Indeed, a stress-induced, rapid increase in the concentration of cytosolic Ca²⁺ has been proposed to trigger altered gene expression not only in response to mechanostimulation but also to myriad biotic and abiotic stresses (Knight, 2000).


Other features that have been proposed to be linked to the initial events of mechanoperception include changes in reactive oxygen species (ROS; Yahraus et al., 1995; Gus-Mayer et al., 1998) that might in turn affect ROS-gated Ca²⁺ channels (Mori and Schroeder, 2004), and ion fluxes at the plasma membrane (Monshausen and Sievers, 1998; Fasano et al., 2001). However, in all these cases, a lack of data on the rapid cellular responses that are induced by or accompany the initial Ca²⁺ increase has limited our understanding of mechanoperception. We therefore monitored the initial cellular events triggered by mechanical

¹ Address correspondence to monshausen@wisc.edu.

² Current address: Swarthmore College, 500 College Avenue, Swarthmore, PA 19081-1397.

The author responsible for distribution of materials integral to the findings presented in this article in accordance with the policy described in the Instructions for Authors (www.plantcell.org) is: Gabriele B. Monshausen (monshausen@wisc.edu).

 Some figures in this article are displayed in color online but in black and white in the print edition.

 Online version contains Web-only data.

www.plantcell.org/cgi/doi/10.1105/tpc.109.068395

stimulation of the root of *Arabidopsis thaliana* to define possible rapid processes activated by mechanical signals at the cell surface. We report that while different types of mechanical stimuli all elicit the elevation of cytosolic Ca^{2+} , the signature of these Ca^{2+} signals is stimulus specific. These Ca^{2+} increases then trigger transient changes in pH and extracellular ROS, the kinetics of which closely mimic the Ca^{2+} signature. Importantly, this Ca^{2+} -dependent signaling pathway is not just triggered by exogenous mechanical perturbation but is also activated in response to endogenously generated mechanical forces. We speculate that this signaling pathway is intimately involved in modulating cell wall characteristics to counteract mechanical stress.

RESULTS

Cytosolic Ca^{2+} Transients Are Triggered by Mechanical Stimulation of the *Arabidopsis* Root

It has previously been demonstrated that mechanical stimulation triggers transient elevations in cytosolic Ca^{2+} (Knight et al., 1991; Legue et al., 1997), but whether there is a relationship between the signature of the elicited Ca^{2+} signal and the type of mechanical stress imposed has yet to be defined. We used the Foerster resonance energy transfer (FRET)-based Ca^{2+} sensor YC3.6 (Nagai et al., 2004; Monshausen et al., 2008a) to noninvasively, and with cellular resolution, monitor and compare the stimulus-specific Ca^{2+} changes triggered by (1) touching an individual root epidermal cell, (2) bending a root, and (3) the mechanical stresses generated endogenously in the root during a thigmotropic growth response.

Point contacts to the surface of the plant have been proposed to represent signals related to fungal penetration or herbivore attack (Hardham et al., 2008). We found that mechanically perturbing a single root epidermal cell with a glass micropipette elicited an increase in cytosolic Ca^{2+} at the site of touch within 1 to 18 s after initiation of the stimulus, with initiating root hairs responding more quickly (6 ± 2.7 s, $n = 11$) than other sites on the root epidermis (12.6 ± 3.7 s, $n = 18$). Once triggered, the Ca^{2+} elevation spread throughout the cytoplasm and nucleus over the course of 2 to 10 s and subsequently dissipated (Figures 1A and 2A; see Supplemental Figure 1 online). This transient and monophasic Ca^{2+} increase was abolished by a brief (2 to 5 min) pretreatment with blockers of Ca^{2+} permeable channels, such as La^{3+} or Gd^{3+} (see Supplemental Figures 2A and 2B online), suggesting that the rise in cytosolic Ca^{2+} levels required the influx of Ca^{2+} from the extracellular space across the plasma membrane.

In contrast with the highly localized mechanical perturbation described above, bending of an organ differentially affects entire tissues and is likely to occur in aerial parts of the plant during, for example, wind stress, or in roots during the growth response to obstacles in the soil (see below). Such a stimulus leads to stretching of cells on the convex side of the curve while compressing cells on the concave side. To impose a bend on roots of *Arabidopsis* seedlings, we immobilized the base of the root in agarose and flexed the exposed part of the root with the

aid of a glass capillary. Bending the organ to a final angle of 40° to 90° was accomplished within ≤ 8 s and resulted in stretching of epidermal cells by up to 10% in length on the convex side. Cytosolic Ca^{2+} levels in these cells rose within 1 s of the start of bending, well before the final angle was achieved (Figures 1B and 2B; see Supplemental Movie 1 online). This initial elevation peaked after 4.6 ± 1.8 s but was then followed by a smaller second peak within 36.6 ± 6.7 s ($n = 11$; Figure 2B). Interestingly, this biphasic Ca^{2+} transient was elicited by bending stimuli of both short (≤ 12 s) and long (> 2 min) duration (i.e., the second phase of the Ca^{2+} transient occurred even when the bend had already been released and the root had straightened) (see Supplemental Figures 3A and 3B online). Biphasic responses were also observed when roots were bent to a shallower angle of 13° to 20° , though the second peak was strongly attenuated (see Supplemental Figure 3C online). By contrast, compression of cells on the concave side triggered either no detectable (three out of eight measurements; see Supplemental Figure 4 online) or a much lower monophasic Ca^{2+} elevation (Figure 2B). Intriguingly, subsequent release of this compression resulted in a strong, but consistently monophasic rise in Ca^{2+} , but only in those cases where the bend had been sustained for 1 to 2 min (see Supplemental Figure 4 online). Consistent with the characteristics of the localized touch stimulation described above, pretreatment with La^{3+} also abolished both phases of these bending-induced Ca^{2+} elevations (see Supplemental Figure 2C online).

Both the touch and bending experiments described above represent the imposition of an exogenous stimulus. We therefore asked whether the endogenous mechanical forces generated by growth were capable of eliciting similar Ca^{2+} signals. Roots encountering an impenetrable obstacle show a characteristic thigmotropic growth response, bending first in the central/proximal elongation zone and subsequently producing a second curvature in the distal elongation zone that represents a combination of thigmotropic and gravitropic responses (Massa and Gilroy, 2003). High-resolution measurements of the development of the initial bend demonstrated that when a root encountered a barrier at a right angle, the position of the root tip initially changed very little as the root pressed against the obstacle (Figure 1C; see Supplemental Movie 2 and Supplemental Figure 5 online). This was followed by release of the accumulated strain as a slippage of the root tip to the side, producing a bend in the basal elongation zone. Root slippage was characterized by a rapid increase in root tip angle for up to 7 min, after which the tip angle changed more slowly (see Supplemental Figure 5 online). These results suggest that extension growth stored while the root pressed against the obstacle was suddenly released during the period of sideways slippage.

As the speed and localization of bending during slippage was reminiscent of the bends we imposed with a glass capillary (see above), we measured cytosolic Ca^{2+} levels in YC3.6-expressing *Arabidopsis* roots encountering a barrier using vertical stage confocal microscopy. While we were unable to detect changes in cytosolic Ca^{2+} in the root elongation zone during the initial phase of contact with the barrier, there was a sudden increase in Ca^{2+} during the phase of slippage (Figures 1C and 2C; see Supplemental Movie 3 online). In the basal elongation zone, Ca^{2+} levels

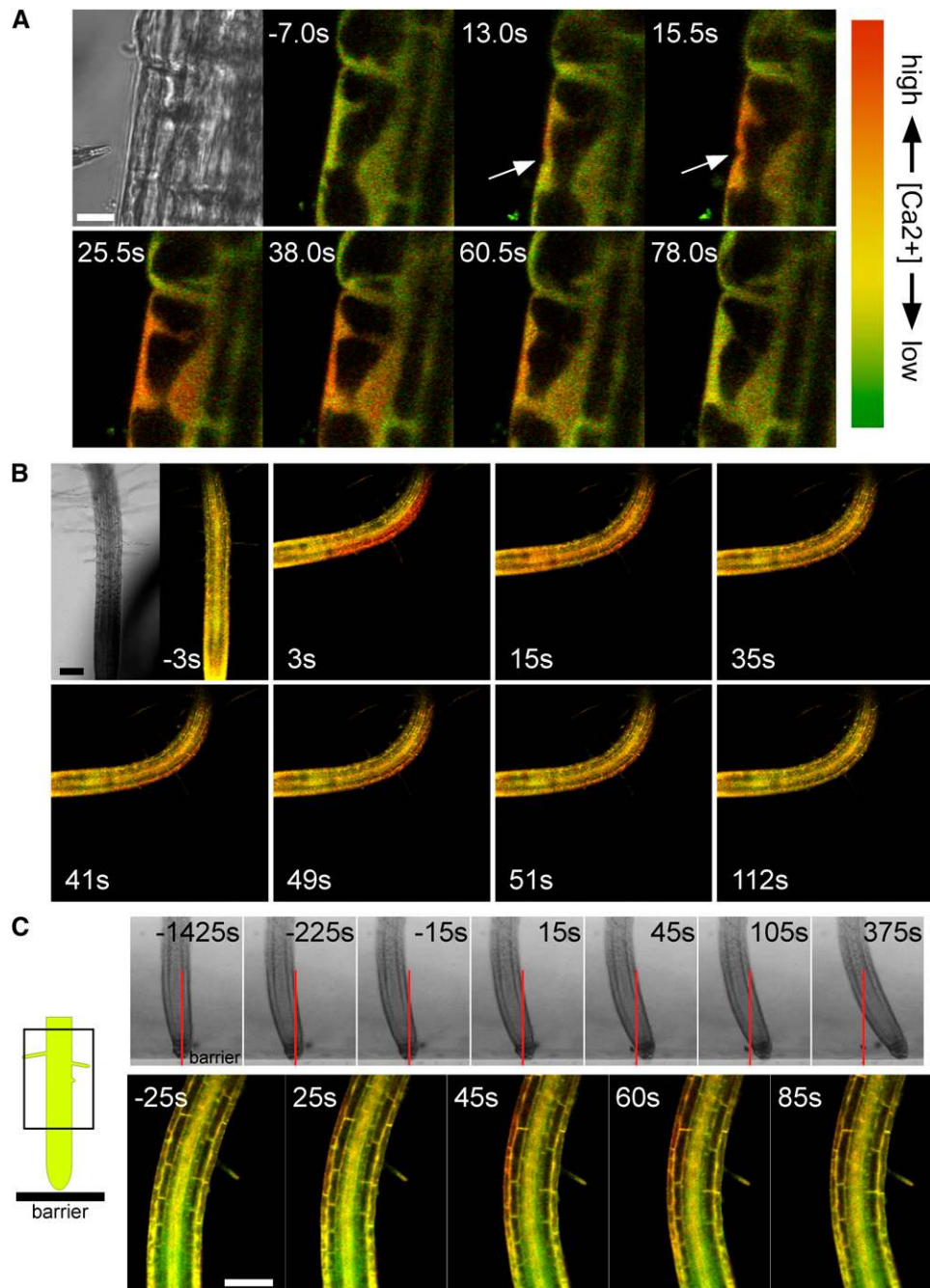


Figure 1. Changes in Cytosolic Ca²⁺ Levels in Response to Mechanical Stimulation Monitored in *Arabidopsis* Roots Expressing YC3.6.

(A) Transient elevation of cytosolic Ca²⁺ triggered by a localized touch stimulus. The first panel shows a bright-field image of a root epidermal cell about to be stimulated with the micropipette touch probe. The sequence of fluorescence images was taken during mechanical stimulation (arrows) of the same cell. Numbers represent time after the start of the touch stimulus in seconds. A red shift in signal reflects an increase in cytosolic Ca²⁺. While the exact strength of the stimulus could not be determined under these conditions, it was sufficient to indent the cell surface, as seen in images taken at 13 and 15.5 s. Note that the Ca²⁺ concentration rises first in the immediate vicinity of the touch site and then spreads throughout the cytoplasm and nucleus. Bar = 10 μm. Representative of *n* > 10 measurements.

(B) Transient elevation of cytosolic Ca²⁺ triggered by bending a root. The first panel shows a bright-field image of the root prior to the bending stimulus. The glass capillary used to bend the root can be seen to the right of the root. The sequence of fluorescence images was taken during mechanical stimulation. Numbers represent time after the start of bending in seconds. A red shift in signal reflects an increase in cytosolic Ca²⁺. Note that the Ca²⁺ concentration increases most strongly in the epidermis and inner tissues of the convex side of the bent root. The complete sequence of images is shown in Supplemental Movie 1 online. Bar = 100 μm. Representative of *n* = 11 measurements.

transiently rose on the convex, stretched side of the developing bend, whereas no Ca^{2+} elevation was detectable on the concave side of the root.

Intra- and Extracellular pH Changes Associated with Touch Stimulation

It has previously been shown that mechanical perturbation of suspension-cultured cells triggers an increase in extracellular pH within 10 min (Gao et al., 2007). Capitalizing on the high sensitivity and wide pH measurement range of proton-selective microelectrodes, we monitored extracellular pH at the root surface during touch stimulation with high temporal resolution. Figure 3A shows that upon contact with the microelectrode (used for both pH recording and as the touch stimulation probe), epidermal cells of the elongation and mature zone consistently exhibited an extracellular pH increase, with surface alkalinizations of up to three pH units within a few seconds.

To improve the spatial resolution of these measurements, we used an imaging approach described previously for use with root hairs (Monshausen et al., 2007). In brief, the medium surrounding the root was supplemented with the pH sensor fluorescein conjugated to a 10-kD dextran. Confocal imaging of a thin plane of fluorescence around the root could then be converted to a two-dimensional map of extracellular pH changes. Figure 3B shows that with this technique, rapid and large alterations in pH could be detected upon touch stimulation, similar to those reported by the microelectrode approach. However, the imaging revealed that these pH changes were localized to the region of the cell in close proximity to that in contact with the stimulation probe. These pH changes did not spread across the surface of the stimulated cell or appear on adjacent cells. Repeated stimulation of the same cell indicated there was no clear refractory period for this response down to 20-s intervals between stimuli, which represented the minimum interval for a touch-induced extracellular pH increase to show a clear falling phase once it was triggered (see Supplemental Figure 6 online) and so the minimum period in which a refractory period could have been resolved.

To determine whether these large apoplastic pH changes were accompanied by equivalent changes in cytosolic pH, we monitored transgenic *Arabidopsis* seedlings expressing a soluble pH-sensitive variant of green fluorescent protein (GFP) (Monshausen et al., 2007), which allowed us to ratio-image cytosolic pH simultaneously with extracellular pH. Such analysis revealed that me-

chanical stimulation triggered changes in cytoplasmic pH, with a transient acidification occurring concomitantly and in phase with the alkalinization of the cell surface (Figures 3B and 3C; see Supplemental Movie 4 online).

Mechanical Bending of the *Arabidopsis* Root Triggers a Biphasic Elevation in Extracellular pH

Similar to the effect of localized touch stimulation on extracellular pH fluxes described above, bending a root in the basal elongation/root hair zone using a glass capillary resulted in a rapid burst of extracellular alkalinization (Figures 4A and 4B), indicating that mechanical stresses at the organ/tissue level also trigger pH responses. The alkalinization was localized to the convex side of the bend where the tissue was stretched. Little or no pH change was observed on the concave side of the root (Figure 4B, inset). Similar to the Ca^{2+} transients described above, both short and sustained stimulations triggered a biphasic extracellular alkalinization response, with a first pH peak occurring after 10.1 ± 1.9 s and a second peak within 43.7 ± 6.9 s ($n = 11$; Figure 4B).

To investigate whether the forces generated by growth could also trigger such a pH response, we again used the barrier assay. Once the vertically growing root had encountered the barrier and started to slip sideways, the rapid curvature development in the elongation zone was accompanied by an alkalinization of the root surface on the stretched convex side of the bend (Figures 5A and 5B; see Supplemental Movie 5 online). No change in surface pH was observed on the concave side of the bend.

Cell Wall-Localized ROS Production Associated with Mechanical Stimulation

To measure extracellular ROS production during mechanical stimulation, we employed an imaging approach described previously using OxyBURST Green $\text{H}_2\text{HFF-BSA}$ (Monshausen et al., 2007). This impermeant sensor becomes fluorescent upon oxidation by ROS and so extracellular ROS production can be monitored by the increase in OxyBURST fluorescence. When *Arabidopsis* seedlings were treated with this sensor, ROS-dependent fluorescence around the elongation and mature zone was clearly evident within <1 min of application of the probe, demonstrating constitutive ROS production in this part of the root (see Supplemental Figure 7 online). However, perturbing initiating root hairs with a glass micropipette resulted in a rapid (within 9 s) increase of fluorescence intensity at the cell surface

Figure 1. (continued).

(C) Transient elevation of cytosolic Ca^{2+} triggered during the root barrier response. The cartoon on the left shows the vertically growing root as it approaches an impenetrable obstacle (coverglass barrier). Top panels: Bright-field images of a root encountering a barrier. As the root encounters the barrier (at the position marked by the red line), it first presses against the obstacle and finally slides to the side, stretching cells on the convex side of the developing bend. Numbers represent time after the start of slippage, which occurred 25 min after first contact was made with the barrier. The complete sequence of images is shown in Supplemental Movie 2 online. Analysis of root tip angles and displacement along the barrier is shown in Supplemental Figure 5 online (bottom panel). Lower panels: Fluorescence images of a root after it has encountered a barrier. The imaged root region corresponds to the boxed area depicted in the cartoon. Numbers represent time after the start of slippage. A red shift in signal reflects an increase in cytosolic Ca^{2+} . Note that the Ca^{2+} concentration can be seen to increase in the epidermis and cortex of the convex side of the bend. The complete sequence of images is shown in Supplemental Movie 3 online. Bar = 100 μm . Representative of $n = 4$ measurements.

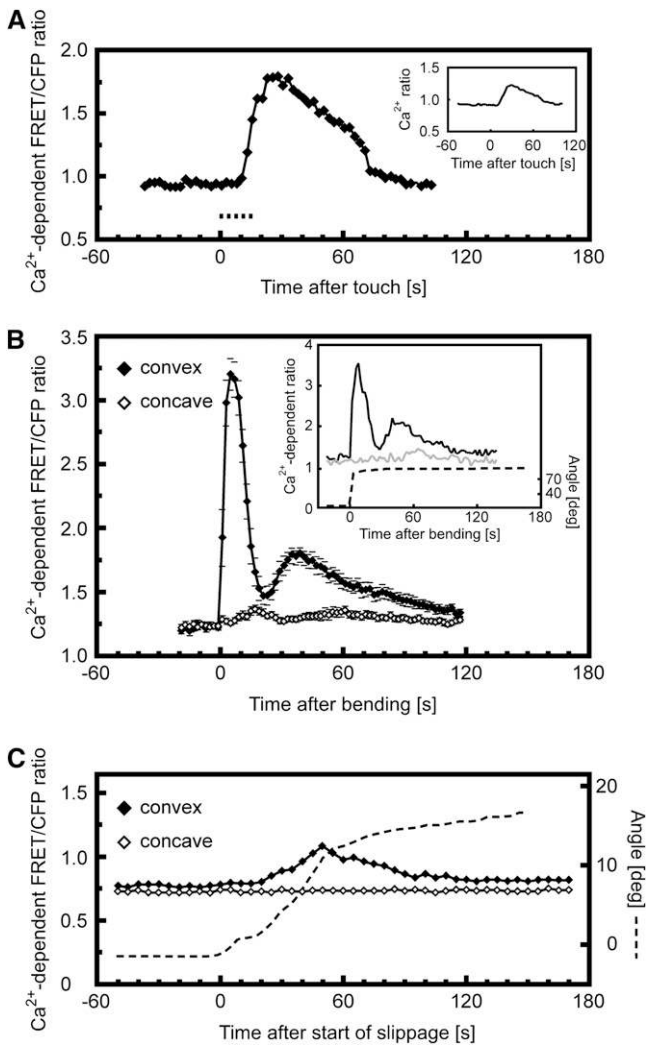


Figure 2. Quantitative Analysis of Cytosolic Ca^{2+} Levels during Mechanical Stimulation.

The regions of interest (ROI) selected for analysis are outlined in Supplemental Figure 1 online.

(A) Touch-induced changes in cytosolic Ca^{2+} in a root epidermal cell at the site of touch. Ca^{2+} -dependent FRET/cyan fluorescent protein (CFP) ratios were measured at the site of touch. An increase in ratio values indicates an increase in cytosolic Ca^{2+} levels. Dashed line indicates duration of touch stimulation. Representative of $n > 10$ measurements. Inset shows touch-induced changes in cytosolic Ca^{2+} averaged across the cytoplasm of the whole cell. Averaging the signal does not alter the monophasic kinetics.

(B) Increase in cytosolic Ca^{2+} levels in response to root bending. The convex side of the root (closed diamonds) showed a clearly biphasic response, whereas a much weaker monophasic response was elicited on the concave side of the bent root (open diamonds). Means \pm SE of 11 bending experiments. Inset shows individual representative example of the Ca^{2+} signal triggered by a sustained bend by $\sim 80^\circ$. The ROIs comprised a single epidermal cell on each side of the root. Black, convex side of the root; gray, concave side; dashed, root angle.

(C) Increase in cytosolic Ca^{2+} levels in response to slippage during the root barrier response. The rise in cytosolic Ca^{2+} levels is restricted to the

(Figures 6A and 6B), suggesting that mechanical stimulation triggered rapid generation of ROS to the cell wall. After ~ 1 min, the OxyBURST signal decreased at the site of touch stimulation (Figures 6A and 6B). As OxyBURST is irreversibly oxidized by ROS to become fluorescent, this reduction in signal most likely represents a combination of decreased ROS production by the cell and diffusion of the activated OxyBURST away from this region. Thus, although the precise kinetics of fluorescence decrease are unlikely to directly reflect the duration of ROS production upon touch stimulation, this assay does show that ROS production in response to touch is transient, terminating within 1 to 2 min of the initial stimulation (Figure 6A). To ensure that these changes in fluorescence reflected ROS production, we confirmed that this touch-induced increase in OxyBURST fluorescence was blocked by addition of the antioxidant ascorbic acid (Figure 6A).

Because irreversibly oxidized OxyBURST accumulates over time, leading to saturation of fluorescence around the root, it was impossible to monitor ROS production during the barrier growth response. However, applying our assay to impose a bend on a root using a glass capillary elicited a rapid asymmetric burst of extracellular ROS, which in 33% of cases was biphasic (Figure 6C; see Supplemental Movie 6 online). We therefore next sought to define the source of this mechanically triggered ROS production.

The NADPH oxidases are a family of membrane-localized enzymes that have been linked to ROS generation in general in plants (Mori and Schroeder, 2004). The NADPH oxidase RBOH C is expressed in roots and has been shown to contribute to ROS production related to root hair elongation (Foreman et al., 2003; Monshausen et al., 2007; Takeda et al., 2008). We therefore investigated touch-related ROS production in the knockout mutant of RBOH C, *rhd2* (Foreman et al., 2003). In contrast with the touch-induced OxyBURST signal seen in wild-type plants, touch stimulation of the initiating root hairs of the *rhd2* mutant did not elicit a detectable alteration in OxyBURST fluorescence intensity (Figure 6B). Thus, in root hairs, RBOH C is likely an important source for the ROS produced in the wall during the rapid oxidative burst triggered by touch.

However, RBOH C seems to play only a minor role in generating the ROS burst elicited by mechanical stimulation elsewhere in the root. Thus, bending *rhd2* roots triggered a strong ROS burst on the convex side of the root, reminiscent of the wild-type response (see Supplemental Figure 8A online). In 50% of the cases, this ROS production was biphasic; indeed, it was more clearly biphasic in *rhd2* than in the wild type, possibly because wild-type roots with root hairs have higher baseline ROS generation, which partially masks these subtle changes in the kinetics of ROS production. This observation suggests that the oxidative environment of the root is predominantly regulated by other ROS-producing enzymes. We have previously demonstrated that the root hair phenotype of *rhd2* can be rescued by growth at

convex side of the developing bend. Dashed line indicates angle of the root as its tip slides along the barrier. Representative of $n = 4$ measurements.

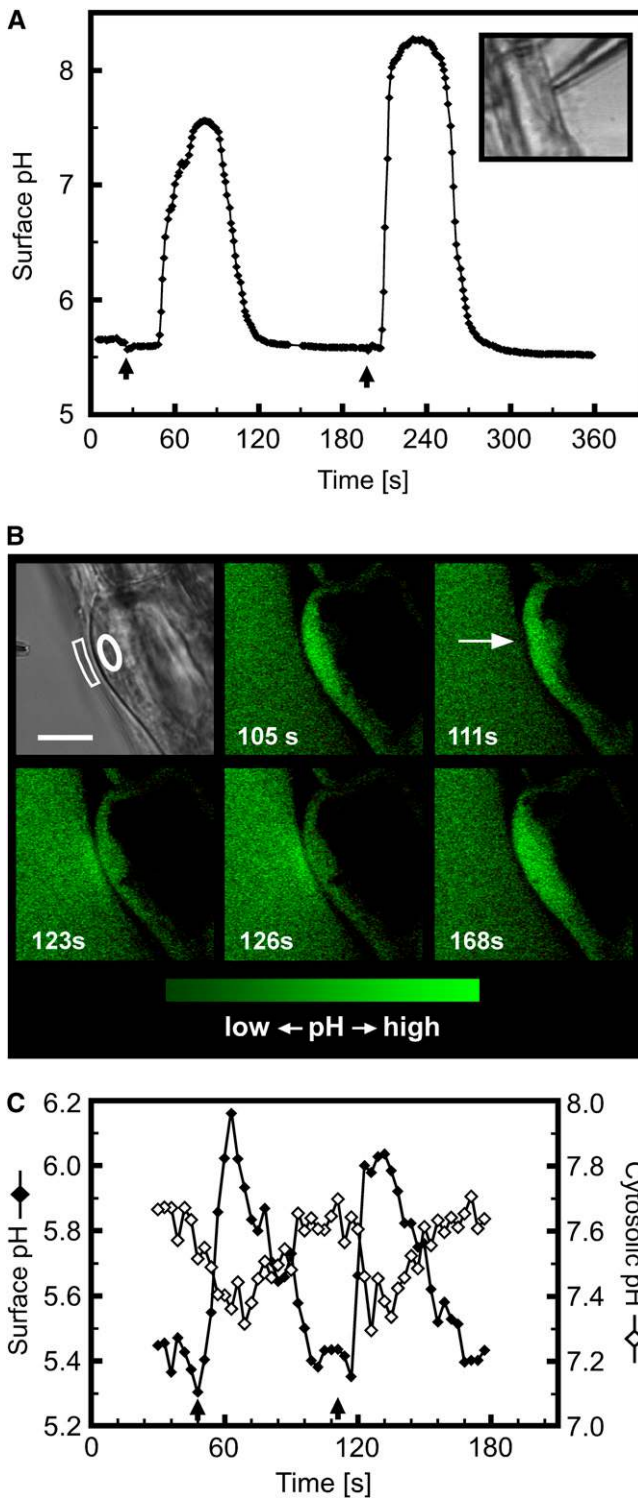


Figure 3. Touch-Induced Changes in Extracellular and Cytosolic pH of Root Epidermal Cells.

(A) The wide measurement range of proton-selective microelectrodes revealed that touch can trigger cell surface alkalization by more than 2.5 pH units in a few seconds. Arrows indicate the start of a touch

elevated pH. In *rhd2* roots grown in the high pH designed to rescue the defective root hair phenotype (Monshausen et al., 2007), a wild-type pattern of ROS-dependent OxyBURST fluorescence was observed along the main root axis (see Supplemental Figure 8B online), consistent with a minor role for RBOH C in ROS production outside of tip-growing root hairs.

Touch-Induced pH Changes and ROS Production Occur Independently of Each Other

The rapid and local effects of touch on pH and ROS production described above led us to ask whether these changes were either coupled or dependent upon one another.

We reasoned that if the touch-induced change in extracellular pH activates RBOH C-dependent ROS production, chemically clamping the pH to similar values as occur during mechanical stimulation should mimic this effect. However, addition of alkaline medium buffered to pH 7.5 with 50 mM HEPES did not result in production of ROS as monitored by OxyBURST fluorescence (Figure 7A). Similarly, buffering the medium to attenuate touch-induced alkalization did not inhibit ROS production (Figure 7A).

To investigate whether ROS play a role in triggering pH changes during the touch response, we treated roots with 100 μ M of the ROS scavenger ascorbic acid. These treated roots still generated strong touch-induced surface alkalization (Figure 7B) but failed to show touch-induced ROS production (Figure 6A). Furthermore, mechanically stimulating initiating root hairs of *rhd2* induced strong transient surface alkalizations (Figure 7C) despite these cells failing to show touch-induced ROS production (Figure 6B). To further test the idea that ROS production and extracellular alkalization are independent processes, we also exposed roots to 10 to 100 μ M H_2O_2 but observed no rapid pH change in the root hair zone related to this treatment (see Supplemental Figure 9 online).

stimulus. Inset shows bright-field image of a root epidermal cell being touched by the tip of a proton-selective microelectrode. Representative of $n > 20$ measurements.

(B) Confocal imaging of touch-induced pH changes using fluorescein-dextran and pH-sensitive GFP as indicators for extracellular and cytosolic pH, respectively. The fluorescein-dextran concentration was titrated so that its signal intensity matched that of the cytosolic pH-sensitive GFP, allowing simultaneous cytosolic and surface pH imaging. The first panel shows a bright-field image of the stimulated cell. The sequence of fluorescence images was taken during mechanical stimulation (arrow) of the same initiating root hair. Increases in signal intensity reflect increases in pH. The complete sequence of images is shown in Supplemental Movie 4 online. Bar in bright-field image = 10 μ m.

(C) Surface (closed diamonds) and cytosolic pH (open diamonds) during repeated mechanical stimulation (arrows) of the trichoblast cell shown in **(B)**. The areas outlined in the bright-field image in **(B)** correspond to those areas from which the measurements were taken.

Note that data points in **(C)** and fluorescence images **(B)** are on the same time scale. Representative of $n = 13$.

[See online article for color version of this figure.]

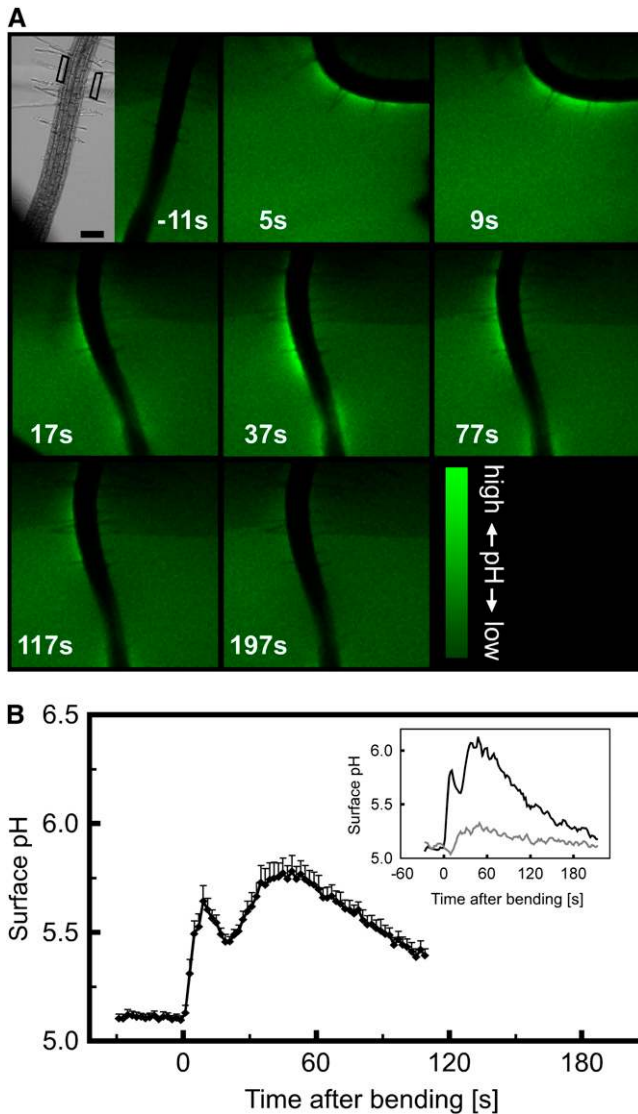


Figure 4. Bending-Induced Increase in Root Surface pH.

(A) Confocal imaging of root surface pH in response to a bending stimulus. The bright-field image shows the root prior to bending with the aid of a glass capillary, seen on the left. The sequence of fluorescence images was taken during mechanical stimulation. The root was incubated in medium containing the pH indicator fluorescein-dextran, which shows increased signal intensity as the pH rises. Numbers represent time after the start of bending in seconds. Note that the pH increases most strongly on the convex side of the bent root. Bar = 100 μm . Representative of $n = 12$ measurements.

(B) Quantitative analysis of the bending-induced, biphasic surface pH increase on the convex side of the root. Means \pm SE of 12 bending experiments. Inset shows individual representative example of pH changes measured in the ROIs along the convex (black) and concave (gray) side of the root outlined in **(A)**.

[See online article for color version of this figure.]

Ca²⁺ Regulation of pH Changes and ROS Production

As described above, mechanical stimulation of the *Arabidopsis* root is related to elevations in cytoplasmic Ca²⁺, the kinetics of which are very similar to mechanically triggered pH and ROS changes (cf. Figures 2 to 6). We therefore next investigated the potential role for Ca²⁺ in a signal transduction pathway activating proton transport and/or ROS generation at the plasma membrane.

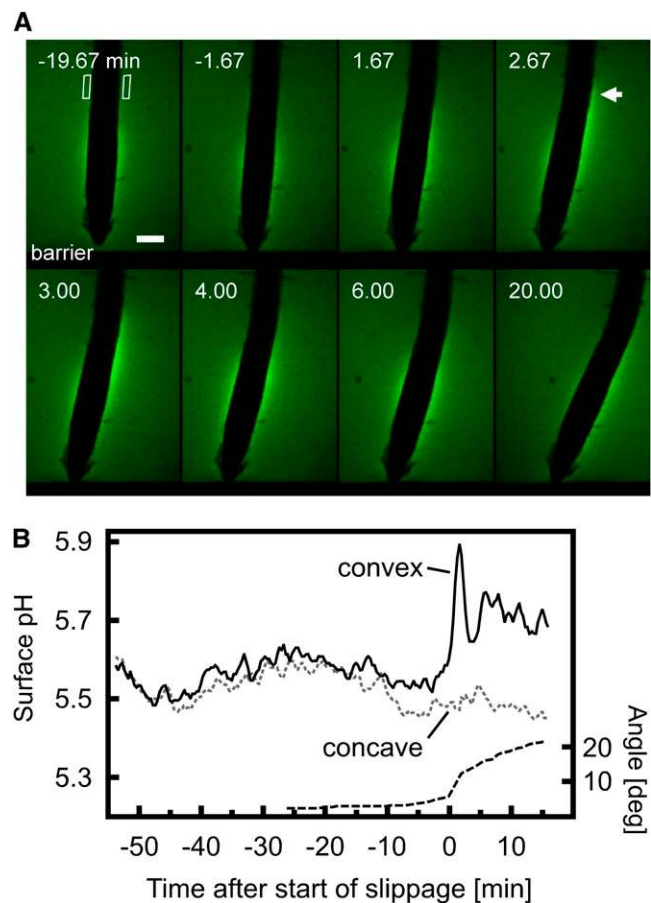


Figure 5. Surface pH Changes during the Root Barrier Response.

(A) As the root grows through agarose containing the pH indicator fluorescein-dextran, it encounters the barrier and subsequently slides to the side, stretching cells on the convex side of the developing bend. Numbers represent time after the start of slippage. Increased signal intensity reflects a rise in pH. Note that while this root initially shows a fairly symmetrical pH profile, the surface pH quickly increases on the convex side of the basal elongation zone where a bend forms during slippage (arrow). The complete sequence of images is shown in Supplemental Movie 5 online. Bar = 100 μm . Representative of $n = 7$ measurements.

(B) Quantitative analysis of pH changes measured in the ROIs along the convex (black) and concave (gray dashed) side of the root outlined in **(A)**. Dashed line indicates root tip angle.

[See online article for color version of this figure.]

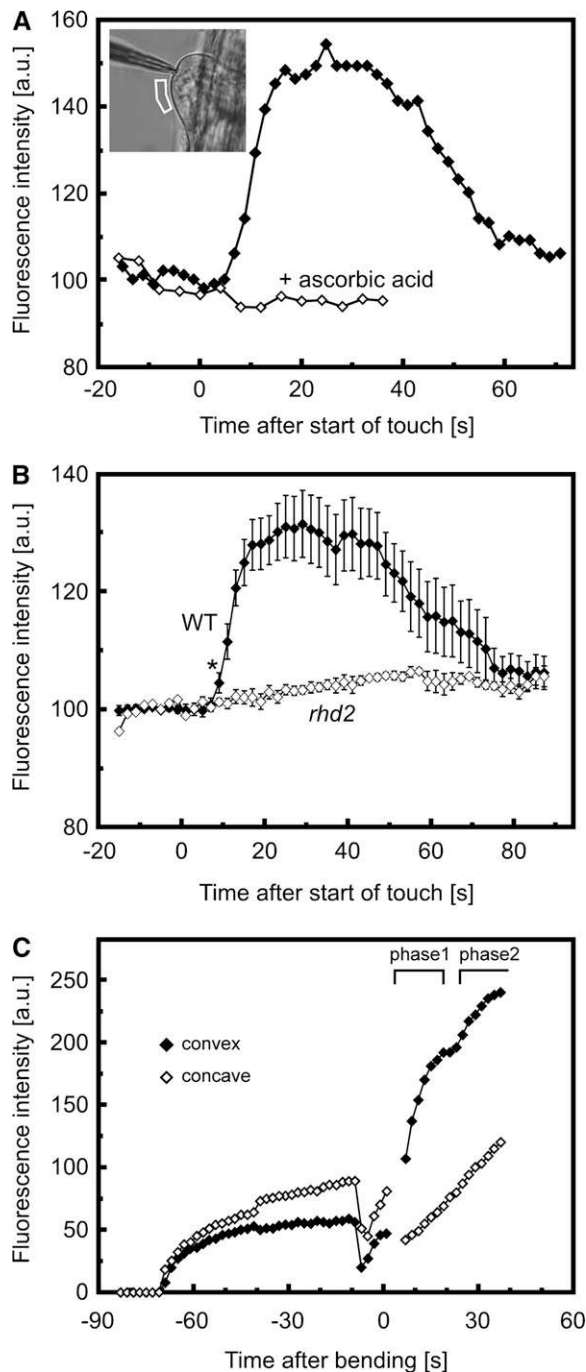


Figure 6. Effect of Mechanical Stimulation on Extracellular ROS Production of Roots.

Because OxyBURST is irreversibly oxidized by ROS to become fluorescent, the measured fluorescence intensity reflects a combination of accumulated ROS production and diffusion. Assuming that the diffusion rate is constant, no change in fluorescence intensity indicates that OxyBURST is being oxidized at the same rate as it diffuses away from the root; an increase in fluorescence reflects a higher rate of OxyBURST oxidation (i.e., ROS production) relative to diffusion; a reduction in fluorescence indicates that the rate of OxyBURST oxidation (ROS

production) has decreased, but the precise kinetics of the loss in fluorescence will reflect contributions from both reduced ROS production and diffusion of the accumulated fluorescent OxyBURST from the root. (A) Effect of touch on extracellular ROS and inhibition of touch-induced ROS production by 100 μ M ascorbic acid. For touch, ROS-dependent OxyBURST fluorescence was measured at the surface of the cell, as indicated in the inset image. Note that in the presence of the ROS scavenger ascorbic acid, touch stimulation did not elicit any detectable increase in fluorescence. Representative of $n \geq 9$ separate experiments. a.u., arbitrary units. (B) Effect of touch on ROS production in the wild type and the *rhd2* mutant. Note that while initiating root hairs of the wild type show a strong increase in ROS production upon a touch stimulus, no such response is detectable in *rhd2*. Results represent mean \pm SE of $n = 10$ (wild type) and $n = 7$ (*rhd2*) measurements. Asterisk indicates fluorescence intensity becoming significantly different from prestimulus intensity at 9 s (t test, $P < 0.05$). (C) Effect of bending on root extracellular ROS production. OxyBURST was added to the medium at -70 s, and ROS-dependent accumulation of fluorescence at the root surface was monitored. At -8 s, the medium was gently mixed by pipetting to dissipate the fluorescence gradient around the root, after which the root was bent (0 s). Note the strong increase in fluorescence asymmetry after the bending stimulus, indicating enhanced ROS production on the convex side of the root. A clear asymmetry was observed in six of nine experiments, with two roots showing the possibly biphasic ROS increase depicted here. A complete sequence of fluorescence images of root bending is shown in Supplemental Movie 6 online.

DISCUSSION

Mechanical Perturbation and Ca^{2+} Signature

The cytosolic concentration of Ca^{2+} rises in response to a wide range of stimuli, consistent with the role of Ca^{2+} as a ubiquitous second messenger in plants. However, a pressing question remains as to whether and how such changes in Ca^{2+} levels

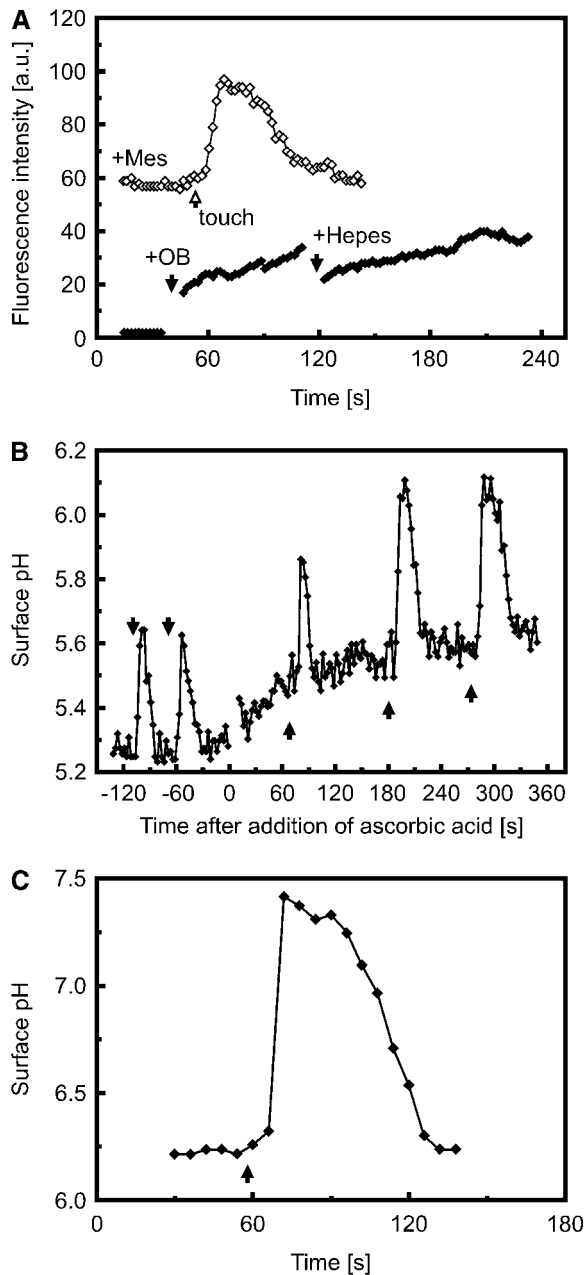


Figure 7. pH Changes and ROS Production Occur Independently of Each Other.

(A) ROS production is independent of extracellular pH changes. Closed diamonds: Extracellular ROS production as monitored by OxyBURST (OB) fluorescence is not affected by a sudden exposure of the root to high extracellular pH (10 mM HEPES, pH 7.5). OxyBURST (200 μ L) was added to the cuvette at \sim 40 s (first black arrow). An additional 200 μ L of 20 mM HEPES + OxyBURST were added at \sim 120 s (second black arrow) for a final concentration of 10 mM HEPES. Open diamonds: Touch-induced ROS production as monitored by OxyBURST fluorescence is not inhibited by buffering the medium with 10 mM MES, pH 6.0. Touch stimulation is indicated by the arrow. Representatives of $n = 3$ measurements, respectively.

(B) and **(C)** Touch-induced extracellular alkalization is not inhibited by

encode information that can be deciphered by plants to initiate stimulus-specific responses (McAinsh and Pittman, 2009). Previous studies have established that mechanical stimulation elicits a transient increase in cytosolic Ca^{2+} and that tissue sensitivity and stimulus intensity can affect the duration and amplitude of this Ca^{2+} transient (e.g., Knight et al., 1991; Haley et al., 1995; Legue et al., 1997). However, our findings indicate that there are not only quantitative but also qualitative differences between Ca^{2+} responses triggered by distinct mechanical perturbations (Figures 1 and 2). Thus, we observed that a strictly localized deformation of the cell surface, such as is thought to occur during pathogen entry (Hardham et al., 2008), provoked a monophasic Ca^{2+} increase, which was initiated at the site of touch and then spread throughout the cytoplasm. By contrast, tissue-wide tensile stresses imposed by bending a root consistently elicited a biphasic Ca^{2+} response in cells under tension, but not in those under compression. While compression of cells during bending triggered only weak transient Ca^{2+} elevations, the release of compression was accompanied by a strong monophasic Ca^{2+} increase if compression had been sustained for several minutes (see Supplemental Figure 3 online).

Critically, Ca^{2+} changes could not only be imposed experimentally by manually manipulating the root, but equivalent changes occurred in response to endogenously generated forces. Thus, Ca^{2+} increases were observed in cells stretched as part of the response to encountering a barrier to growth (Figures 1 and 2). These observations suggest that mechanically induced Ca^{2+} signals may be an intrinsic component of the stresses inherent in turgor-driven growth.

Our results suggest that Ca^{2+} influx across the plasma membrane is a requirement for both the monophasic and biphasic Ca^{2+} elevations. Thus, a brief pretreatment with the Ca^{2+} channel blockers La^{3+} or Gd^{3+} completely inhibited all mechanically induced Ca^{2+} responses (see Supplemental Figure 2 online). In our hands, these blockers were effective at consistently abolishing the Ca^{2+} response only at extracellular Ca^{2+} concentrations of ≤ 0.2 mM. At 1 mM Ca^{2+} , bending experiments elicited a (albeit attenuated) Ca^{2+} increase even in the presence of 1 mM LaCl_3 . This observation may explain the conflicting results of Legue et al. (1997), who detected no clear La^{3+} inhibition of touch-induced Ca^{2+} increases in roots under conditions of ≥ 1 mM extracellular Ca^{2+} and so concluded that mechanical stimulation triggers Ca^{2+} release primarily from internal stores. While plasma membrane Ca^{2+} permeable channels likely mediate the initial rise in cytosolic Ca^{2+} , their activation may not be sufficient to account for the persistence of the Ca^{2+} signal or its migration throughout the cytoplasm (Figures 1 and 2). The high Ca^{2+} -buffering capacity of the cytoplasm attenuates the magnitude of Ca^{2+} elevations and diffusion of Ca^{2+} within the cell, suggesting that the propagation of Ca^{2+} increases away from the plasma membrane is likely to be sustained by release of Ca^{2+} from internal stores.

scavenging extracellular ROS with 100 μ M ascorbic acid **(B)** or by loss of touch-induced ROS production in the *rhd2* mutant background **(C)**. Arrows indicate touch stimulation. Representative of $n > 10$ measurements.

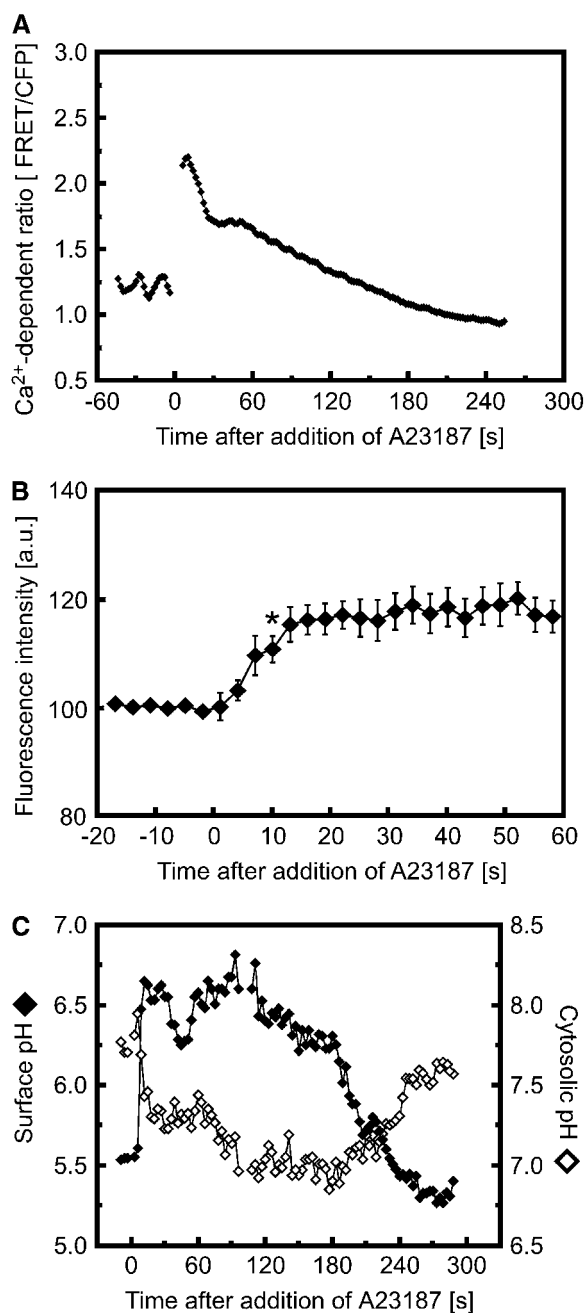


Figure 8. Effect of the Ca²⁺ ionophore A23187 on Cellular Ca²⁺, ROS Production, and pH.

(A) Treatment with 10 μ M A23187 triggers a rapid increase in cytosolic Ca²⁺ levels in *Arabidopsis* root hairs expressing YC3.6. Representative of $n = 7$ experiments.

(B) Treatment with 10 μ M A23187 triggers a rapid increase in ROS-dependent OxyBURST fluorescence at the surface of initiating *Arabidopsis* root hairs. Data are means \pm SE of four separate experiments. Asterisk indicates fluorescence intensity becoming significantly different from prestimulus intensity at 10 s (t test, $P < 0.05$).

(C) Treatment with 10 μ M A23187 triggers a rapid change in extracellular (closed diamonds) and cytosolic (open diamonds) pH. Representative of $n = 8$ experiments.

Ca²⁺-dependent mobilization of Ca²⁺ from intracellular stores has been shown to be crucial for the propagation of Ca²⁺ waves in animal cells, such as neurons and eggs (Berridge, 2002; Galione and Churchill, 2002). Similar mechanisms have been proposed to potentiate Ca²⁺ signals in plants by increasing signal amplitude, duration, and/or distribution leading to modulation of the Ca²⁺ signature (reviewed in McAinsh and Pittman, 2009). The possible presence of diverse mechanoreceptors (reviewed in Monshausen and Gilroy, 2009), whose juxtaposed activation may trigger Ca²⁺ influx through different subsets of plasma membrane channels, may add further flexibility to this signaling system. Differential activation of mechanoreceptors could explain, for example, the dichotomy between Ca²⁺ responses elicited by tension and release of prolonged compression, both of which triggered a strong rapid Ca²⁺ increase, but only one of which was followed by a second slower Ca²⁺ transient (see above). It is also important to note that in addition to blocking Ca²⁺ channel action, high concentrations of La³⁺ have been reported also to affect, for example, anion channel activity (Lewis and Spalding, 1998). Thus, although the inhibitory effects of La³⁺ and Gd³⁺ on mechanically induced Ca²⁺, pH, and ROS changes are strongly suggestive of a role for plasma membrane Ca²⁺ permeable channels in triggering these events, we must await molecular characterization of the mechanism of touch-induced Ca²⁺ entry to be certain of this possibility. Unfortunately other putative Ca²⁺ channel blockers, including up to 1 mM verapamil and nifedipine, have proven ineffective in blocking these mechanically induced Ca²⁺ increases.

Mechanical Stimulation Triggers Ca²⁺-Dependent Changes in Plasma Membrane Proton Fluxes

The Ca²⁺ signals described above appear intimately connected to mechanoperception (Monshausen et al., 2008b). However, while many thigmomorphogenetic responses have been described in exquisite detail (reviewed in Braam, 2005), our understanding of the signaling pathways linking these initial Ca²⁺ signals to downstream transcriptional or developmental responses is still fragmentary.

Our results show that in addition to generating rapid Ca²⁺ signals, intact seedlings of *Arabidopsis* respond to mechanical stimulation with rapid and substantial changes in cytoplasmic and extracellular pH (Figures 3 to 5). Both the timing and amplitude of these changes closely mimicked those of mechanically triggered Ca²⁺ transients (Figures 1 to 5), suggesting a relationship between Ca²⁺ and pH changes. Consistent with this idea, pH responses were abolished by pretreatment with the Ca²⁺ channel blockers La³⁺ or Gd³⁺ (Figure 9) but could be induced in the absence of stimulation by artificially elevating Ca²⁺ levels (Figure 8), indicating that Ca²⁺ influx is both necessary and sufficient for triggering pH changes.

Mechanically induced increases in root surface pH appeared to be linked temporally and in magnitude with decreases in cytoplasmic pH, suggesting that extracellular alkalization and cytoplasmic acidification are mechanistically coupled. A similar relationship between cytosolic and wall pH changes has been suggested in growing root hairs and pollen tubes (Messerli and Robinson, 1998; Messerli et al., 1999; Monshausen et al., 2007).

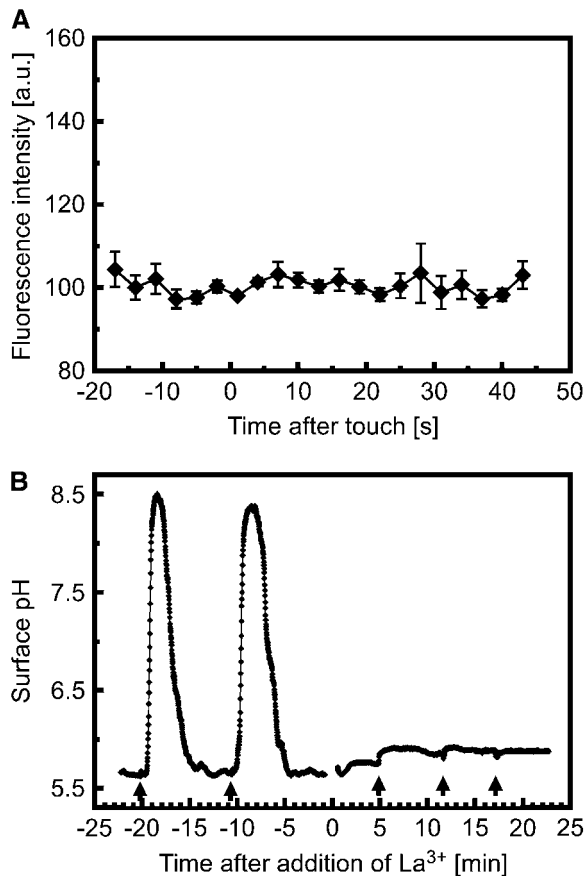


Figure 9. Touch-Induced ROS and pH Changes Are Inhibited by the Ca²⁺ Channel Blocker La³⁺.

(A) Inhibition of touch-induced ROS production by 100 μ M LaCl₃. Data are means \pm SE of five experiments.

(B) Inhibition of touch-induced surface pH changes by 100 μ M LaCl₃. pH was measured at the surface of an atrichoblast in the mature zone of the root using a proton-selective microelectrode. Representative of $n = 12$ separate experiments.

The H⁺-ATPase and plasma membrane ion channels have all been shown to be modulated by cytoplasmic Ca²⁺ levels (Schroeder and Hagiwara, 1989; Hedrich et al., 1990; Kinoshita et al., 1995; Lino et al., 1998), providing possible mechanisms whereby altered Ca²⁺ levels may translate into the changes in plasma membrane H⁺ flux we have observed.

The ability of a cell to rapidly change bulk cytosolic and surface pH has the potential to alter many facets of cell wall and cytoplasmic functions, making pH a strong candidate for propagating signaling information. Indeed, while our measurements show that the surface pH rises by up to 3 units and the bulk cytosol acidifies by 0.4 units within seconds (Figure 3), the shift in proton concentration in the immediate vicinity of the plasma membrane may be even larger. Changes in pH on this scale should dramatically affect the activity of numerous proteins. For example, pH is well characterized as a regulator of plasma membrane transporters (Blatt, 1992; Regenberget al., 1995),

proteins associated with the cytoskeleton (Allwood et al., 2002; Frantz et al., 2008), and aquaporins (Verdoucq et al., 2008). Changes in cytosolic pH will also alter the binding affinity of EF hand-containing Ca²⁺ binding proteins, such as calmodulin (Busa and Nuccitelli, 1984), and pH changes have been shown to modulate gene transcription (Lapous et al., 1998). The alteration of proton fluxes thus represents one mechanism to transduce mechanical perception to the cytosolic activities and transcriptional changes characterized as accompanying mechanoresponses.

Increases in extracellular pH are also expected to regulate a number of enzymes known to affect cell wall rigidity (Price et al., 2003; Bosch and Hepler, 2005; Di Matteo et al., 2005; Parre and Geitmann, 2005; Almagro et al., 2009) and, indeed, have been shown to help stabilize the cell wall of growing root hairs (Monshausen et al., 2007). Such observations suggest a general response that whenever a cell experiences mechanical strain, either generated internally by a burst of expansion (Figure 5; Monshausen et al., 2007) or imposed externally via environmental stress (Figures 3 and 4), it will transiently raise the extracellular pH to secure the cell wall. Thus, a coordinated change in cytosolic and wall pH is likely to have widespread regulatory effects at levels from the modulation of wall structure to cytosolic enzyme activities and gene transcription, providing a mechanism to coordinate the diverse physiological and developmental effects that define the mechanical response system of the plant.

Mechanical Stimulation Triggers Ca²⁺-Dependent Changes in ROS Production

In addition to characterizing the rapid Ca²⁺-dependent pH response, we were also able to directly and noninvasively monitor rapid and transient changes in ROS production associated with root responses to touch stimulation. Mechanical effects on cytosolic ROS levels have been investigated previously by monitoring dichlorofluorescein fluorescence (Yahraus et al., 1995; Gus-Mayer et al., 1998). Using this intracellular probe, it was shown that sustained mechanical stress induces ROS production in suspension cultured soybean (*Glycine max*) and parsley (*Petroselinum crispum*) cells within 4 to 10 min (Yahraus et al., 1995; Gus-Mayer et al., 1998). Our experiments using OxyBURST-BSA demonstrate that in intact root tissue, rapid localized generation of extracellular ROS can be detected within 9 s of a touch stimulus (Figure 6). This ROS burst was sensitive to Ca²⁺ channel blockers (Figure 9) and could be induced by treatment with Ca²⁺ ionophore (Figure 8), indicating that ROS production was also rapidly activated by the touch-associated Ca²⁺ increase. These results are consistent with the described Gd³⁺/La³⁺ sensitivity of the oxidative burst in soybean and parsley suspension cells (Yahraus et al., 1995; Gus-Mayer et al., 1998).

In root hairs, we observed that touch-stimulated ROS production was dependent on RBOHC, an *Arabidopsis* homolog of the phagocyte NADPH oxidase subunit gp91^{phox} (Foreman et al., 2003). Thus, while ROS-dependent fluorescence of OxyBURST-BSA increased strongly within 9 s of touch stimulation, no such increase was ever observed in mechanically stimulated *rhd2*,

an *Arabidopsis* mutant lacking a functional RBOH C (Figure 6). Intriguingly, the ability to bind Ca^{2+} is essential to the activation of RBOH C and D when expressed heterologously in mammalian HEK 293T cells (Ogasawara et al., 2008; Takeda et al., 2008), and our results indicate that such Ca^{2+} -dependent activation of RBOH C also likely occurs in planta. While it seems plausible that similar regulatory mechanisms were responsible for triggering ROS production during root bending, mechanically stimulated ROS production was still seen upon bending *rhd2* roots (see Supplemental Figure 8 online). Of the 10 *RBOH* genes found in the *Arabidopsis* genome, eight are expressed in roots (Sagi and Fluhr, 2006), raising the possibility of a high level of redundancy.

What are the potential targets of ROS generated during responses to mechanical stress? While long-term effects likely include regulation of gene expression (Apel and Hirt, 2004), rapid ROS production to the apoplast should rigidify and strengthen the cell wall through oxidative cross-linking of cell wall components (Campbell and Sederoff, 1996; Brady and Fry, 1997; Kerr and Fry, 2004). Such a role in enhancing cell wall stability is supported by the observation that defects in ROS production lead to bursting of growing root hairs, as does scavenging of

extracellular ROS. Conversely, treatment with exogenous ROS immediately inhibited cellular expansion (Monshausen et al., 2007). Consistent with these ideas, increased production of ROS was shown to protect *Fucus* rhizoids from cell wall rupture during hypoosmotic shock (Coelho et al., 2002). Thus, ROS production may be coordinated with an elevation of apoplastic pH to fortify the wall and so contribute to the reduced stature, slower growth, and increased robustness of plants exposed to mechanical stresses (Mitchell, 1996).

In summary, we have found that distinct mechanical stresses elicit cytosolic Ca^{2+} elevations with stimulus-specific signatures. Based on the pharmacological evidence we have presented, we propose that these Ca^{2+} transients are initiated by Ca^{2+} influx across the plasma membrane. Mechanical stresses also trigger rapid ROS production to the wall and proton influx to the cytoplasm, with concomitant wall alkalization. As these changes closely mimic the kinetics of observed Ca^{2+} transients and are inhibited by blockers of Ca^{2+} influx, we hypothesize that elevation of cytosolic Ca^{2+} levels may regulate ROS generation and proton fluxes. Importantly, we have shown that this signal transduction pathway is not just triggered when mechanical stresses are imposed exogenously, but is potentially part of a

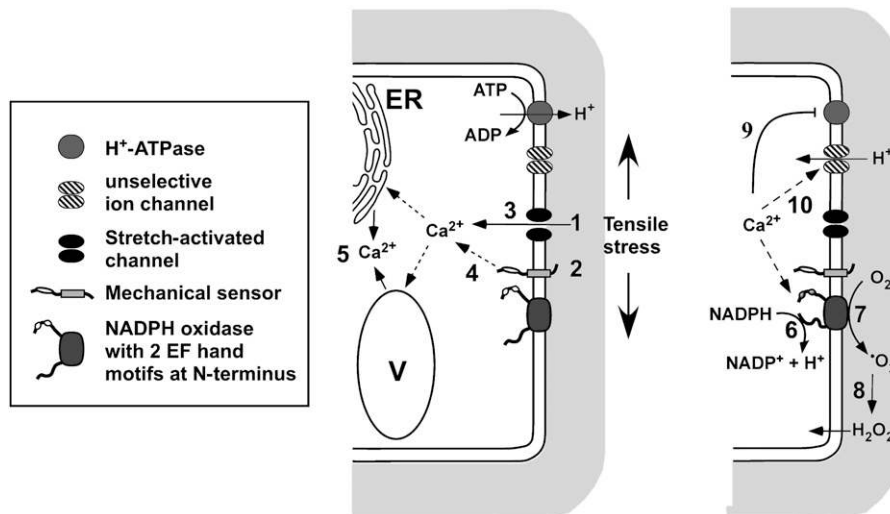


Figure 10. Model of Early Signaling Events upon Mechanical Stimulation.

Plants can be mechanically perturbed exogenously, for example, during wind stress and by obstacles in the soil, but plants also generate mechanical stresses internally, for example, as tissue tension or during cell elongation. Perception of these stresses likely occurs through sensing the deformation of the cell wall and appressed plasma membrane via activation of mechanosensors, such as stretch-gated Ca^{2+} permeable channels (1) and/or putative cell wall integrity sensors (2). This activation leads directly (3) or indirectly (4) to an influx of Ca^{2+} into the cytoplasm. Within the cytoplasm, the Ca^{2+} signal is amplified, for example, through Ca^{2+} -dependent mobilization of Ca^{2+} from internal stores (5). At the plasma membrane, elevated Ca^{2+} levels activate plasma membrane NADPH oxidases through the Ca^{2+} binding EF hand motifs, resulting in NADPH oxidation (6) and extracellular superoxide (ROS) production (7). In the cell wall, superoxide is dismutated to H_2O_2 (8), which can easily diffuse back into the cytoplasm. Elevated Ca^{2+} levels also lead to cytosolic acidification and cell wall alkalization: both Ca^{2+} -dependent activation of NADPH oxidation (6) and inhibition of plasma membrane H^+ ATPases (9) contribute to this pH change; however, the rapidity and magnitude of the pH changes suggest the involvement of other transporters, such as unselective cation or anion channels (10), which may mediate H^+ or OH^- fluxes to quickly alter extra- and intracellular pH. Cytosolic ROS, acidification, and Ca^{2+} increase are all known to elicit signaling events. Similarly, elevated wall pH and ROS are known to rigidify the cell wall matrix. Intriguingly, similar signaling cascades have also been described during defense responses (Garcia-Brugger et al., 2006), suggesting that this suite of coupled changes in cytosolic and wall environment (alterations in ROS, pH, and Ca^{2+}) represents a fundamental response cassette that is used by plants to protect themselves against a range of environmental insults but has also been recruited to monitor and regulate cellular expansion. ER, endoplasmic reticulum; V, vacuole.

plant's response repertoire to the mechanical strain experienced under normal growth conditions (Figure 10). Indeed, elements of this mechanically induced signaling cascade have also been found in tip-growing root hairs and pollen tubes (Messerli and Robinson, 1998; Messerli et al., 1999; Monshausen et al., 2007, 2008a). In these cell types, turgor-driven growth oscillates between rates of accelerated and decelerated elongation. Intriguingly, these growth oscillations, which are likely accompanied by oscillations in mechanical strain, are also tightly correlated with oscillations in Ca^{2+} , pH, and ROS. It therefore seems plausible that a general mechanism for monitoring and responding to strain has been recruited to serve in a negative feedback loop to limit cellular expansion.

METHODS

Plant Material

Surface-sterilized *Arabidopsis thaliana* (Columbia) wild-type and *rhd2* (Foreman et al., 2003) seeds were germinated in Petri dishes on the surface of sterile 1% (w/v) agar containing one-quarter strength Murashige and Skoog basal salt mixture (Sigma-Aldrich) and 1% (w/v) sucrose, pH 5.8. Plants were grown for 4 to 5 d in continuous light at $22 \pm 2^\circ\text{C}$ and mounted in purpose-built chambers as previously described (Monshausen et al., 2007).

Mechanical Stimulation and Inhibitor Studies

Arabidopsis roots were mechanically stimulated following three different protocols: (1) Individual epidermal cells were touched by rubbing a glass micropipette tip along the cell surface using a micromanipulator. (2) Roots were bent in the proximal elongation/mature zone. To impose a bend, the base of the root was immobilized in agarose, and the exposed part of the root was flexed with the aid of a glass capillary. (3) Vertically oriented roots immersed in agarose were grown into a barrier consisting of a piece of coverglass placed perpendicular to the root long axis (see Massa and Gilroy, 2003).

Root tip angles and root growth were analyzed using the Zeiss LSM 510 analytical software. For treatments with the Ca^{2+} ionophore A23187 (0.1% DMSO final concentration), the Ca^{2+} channel blockers Gd^{3+} and La^{3+} , and the ROS scavenger ascorbic acid, roots were either pretreated with the respective compounds for <10 min, or the compound was added during the course of the experiment as indicated in the figure legends.

Electrophysiology

Proton-selective microelectrodes were used to measure extracellular pH at the surface of *Arabidopsis* root hairs and epidermal cells. The preparation of the electrodes and seedling setup have been described previously (Monshausen et al., 2007). Surface pH was monitored by positioning the electrode tip 1 to 2 μm from the cell surface. To administer a touch stimulus, the electrode tip was pushed against and rubbed along the cell surface. Control experiments in medium buffered with 10 mM MES, pH 6, or containing inhibitors, such as 100 μM La^{3+} and Gd^{3+} , showed that contact of the electrode with the cell surface introduced only a minor shift in the measured voltage in the range of <6 mV.

Simultaneous Measurement of Cytosolic and Extracellular pH

Wild-type *Arabidopsis* plants or *Arabidopsis* expressing a pH-sensitive variant of GFP (H148D) were mounted in purpose-built chambers,

bathed in medium containing fluorescein-10 kD dextran (aqueous minimal medium for touch and bending experiments; 1% agarose minimal medium for barrier experiments), and imaged, all as previously described (Monshausen et al., 2007). In brief, the GFP and fluorescein fluorophores were imaged using a Zeiss LSM 510 confocal microscope and alternating 458- and 488-nm excitation, 488-nm dichroic mirror, and 505-nm long-pass emission filter. For touch experiments, a $\times 40$ 1.2 numerical aperture, C-Apochromat, water immersion objective was used. For bending and barrier response experiments, roots were imaged with a $\times 10$ 0.3 numerical aperture Plan-Neofluar objective. For touch and bending experiments, simultaneous bright-field images were collected with each 488-nm excitation scan using the transmission detector. pH measurements during the barrier response were performed by mounting the experimental chamber containing the *Arabidopsis* seedling on a custom-built vertical stage (Kramer, 2004) and redirecting the light path of the LSM 510 to the sample via a custom-built periscope (LSM Technologies) for vertical stage confocal microscopy. Because vertical stage confocal microscopy did not allow for simultaneous acquisition of bright-field images, we obtained high-resolution bright-field images of a root growing into a barrier using a vertical stage Nikon Diaphot TE300 microscope.

Ratio analysis of fluorescence intensities in defined regions of interest was performed using the analytical software of the LSM 510. Extracellular and cytosolic pH measurements were calibrated as described (Monshausen et al., 2007).

Measurement of Cytosolic Ca^{2+} Using Cameleon YC 3.6

Stably transformed *Arabidopsis* expressing the yellow cameleon YC3.6 construct driven by the 35S promoter (35S:YC3.6 in pEarleyGate 100) were imaged using the META detector of the Zeiss LSM 510 confocal microscope as described (Monshausen et al., 2008a). For touch experiments, the $\times 40$ water immersion objective was used; for bending and barrier response experiments, roots were imaged with the $\times 10$ objective described above or a $\times 20$, 0.8 numerical aperture Plan-Apochromat objective. With increasing Ca^{2+} concentration, the cameleon YC3.6 sensor shows an increase in FRET signal and decrease in cyan fluorescent protein fluorescence intensity. Ratio analysis of fluorescence intensities in defined regions of interest was performed using the analytical software of the LSM 510.

Monitoring Extracellular ROS with OxyBURST-BSA

Extracellular release of ROS from *Arabidopsis* roots was monitored using the fluorogenic reagent OxyBURST Green H_2HFF made cell impermeable by conjugation to BSA (Molecular Probes). Roots were incubated in the presence of the fluorogenic reagent (100 $\mu\text{g mL}^{-1}$), and fluorescence accumulation was recorded using the Zeiss LSM 510 laser scanning confocal microscope. The fluorescent oxidized product was excited with the 488-nm line of an argon ion laser. Emission was monitored using a 488-nm primary dichroic mirror and a 505-nm long-pass filter. Fluorescence intensities are presented in arbitrary units. We normalized values by determining the average prestimulus fluorescence intensity for each measurement, calculating the difference between this average and 100 and then adding this difference to all values in the measurement, thereby shifting each curve so that the prestimulus average was now 100 arbitrary units. The exception to this presentation is experiments where measurements started prior to OxyBURST addition; here, presented values reflect absolute pixel intensities measured in each ROI. Because OxyBURST is irreversibly oxidized to a fluorescent product, we could not use this approach to monitor the exact time course of ROS transients. However, OxyBURST did provide a sensitive measure of the onset of ROS production at the cell surface.

Accession Number

Sequence data from this article can be found in the Arabidopsis Genome Initiative or GenBank/EMBL databases under accession number At5g51060 (*Arabidopsis RBOH C*).

Supplemental Data

The following materials are available in the online version of this article.

Supplemental Figure 1. Regions of Interest Selected for Analysis of Ca²⁺-Dependent FRET/CFP Ratios.

Supplemental Figure 2. Inhibition of Mechanically Induced Cytosolic Ca²⁺ Changes by Ca²⁺ Channel Blockers.

Supplemental Figure 3. Increase in Cytosolic Ca²⁺ Levels in Response to Root Mechanical Stimulation.

Supplemental Figure 4. During a Bending Stimulus, Stretching and Release of Compression Trigger Ca²⁺ Signals with Distinct Signatures.

Supplemental Figure 5. Three Examples of *Arabidopsis* Roots Showing the Range of Characteristic Thigmotropic Growth Responses upon Encountering an Impenetrable Barrier.

Supplemental Figure 6. Measurement of Cell Surface pH Changes during Repeated Touch Stimulation.

Supplemental Figure 7. ROS-Dependent OxyBURST Fluorescence Pattern around a Growing *Arabidopsis* Root.

Supplemental Figure 8. Extracellular ROS Pattern around Roots of *rhd2*.

Supplemental Figure 9. Effect of Exogenous ROS on Root Surface pH.

Supplemental Figure 10. Effect of the Ca²⁺ Channel Inhibitor La³⁺ on Bending-Induced ROS and pH Changes.

Supplemental Figure 11. Inhibition of Touch-Induced Surface pH Changes by La³⁺.

Supplemental Movie 1. Transient Elevation of Cytosolic Ca²⁺ Triggered by Bending a Root and Subsequently Releasing the Bend.

Supplemental Movie 2. *Arabidopsis* Roots Showing a Characteristic Thigmotropic Growth Response upon Encountering an Impenetrable Barrier.

Supplemental Movie 3. Transient Elevation of Cytosolic Ca²⁺ Triggered during the Root Barrier Response.

Supplemental Movie 4. Touch-Induced pH Changes in *Arabidopsis* Initiating Root Hair.

Supplemental Movie 5. Vertical Stage Confocal Imaging of Surface pH Changes during the Root Barrier Response.

Supplemental Movie 6. Bend-Induced Asymmetric Increase in Root Extracellular ROS Production.

ACKNOWLEDGMENTS

This work was supported by grants to S.G. (National Science Foundation Grants MCB 0641288 and IBN 03-36738) and G.B.M. (National Science Foundation Grant MCB 0641288). The confocal imaging was performed at the Plant Imaging Center, Department of Botany, University of Wisconsin-Madison.

Received May 5, 2009; revised June 25, 2009; accepted July 14, 2009; published August 4, 2009.

REFERENCES

- Allwood, E.G., Anthony, R.G., Smertenko, A.P., Reichelt, S., Drobak, B.K., Doonan, J.H., Weeds, A.G., and Hussey, P.J. (2002). Regulation of the pollen-specific actin-depolymerizing factor LIADF1. *Plant Cell* **14**: 2915–2927.
- Almagro, L., Gomez Ros, L.V., Belchi-Navarro, S., Bru, R., Ros Barcelo, A., and Pedreno, M.A. (2009). Class III peroxidases in plant defence reactions. *J. Exp. Bot.* **60**: 377–390.
- Apel, K., and Hirt, H. (2004). Reactive oxygen species: Metabolism, oxidative stress, and signal transduction. *Annu. Rev. Plant Biol.* **55**: 373–399.
- Berridge, M.J. (2002). The endoplasmic reticulum: A multifunctional signaling organelle. *Cell Calcium* **32**: 235–249.
- Blatt, M.R. (1992). K⁺ channels of stomatal guard cells. Characteristics of the inward rectifier and its control by pH. *J. Gen. Physiol.* **99**: 615–644.
- Bosch, M., and Hepler, P.K. (2005). Pectin methylesterases and pectin dynamics in pollen tubes. *Plant Cell* **17**: 3219–3226.
- Braam, J. (2005). In touch: Plant responses to mechanical stimuli. *New Phytol.* **165**: 373–389.
- Braam, J., and Davis, R.W. (1990). Rain-, wind-, and touch-induced expression of calmodulin and calmodulin-related genes in *Arabidopsis*. *Cell* **60**: 357–364.
- Braam, J., Sistrunk, M.L., Polisensky, D.H., Xu, W., Purugganan, M.M., Antosiewicz, D.M., Campbell, P., and Johnson, K.A. (1997). Plant responses to environmental stress: Regulation and functions of the *Arabidopsis* TCH genes. *Planta* **203**: S35–S41.
- Brady, J.D., and Fry, S.C. (1997). Formation of di-isodityrosine and loss of isodityrosine in the cell walls of tomato cell-suspension cultures treated with fungal elicitors or H₂O₂. *Plant Physiol.* **115**: 87–92.
- Busa, W.B., and Nuccitelli, R. (1984). Metabolic regulation via intracellular pH. *Am. J. Physiol.* **246**: R409–R438.
- Campbell, M.M., and Sederoff, R.R. (1996). Variation in lignin content and composition - Mechanisms of control and implications for the genetic improvement of plants. *Plant Physiol.* **110**: 3–13.
- Coelho, S.M., Taylor, A.R., Ryan, K.P., Sousa-Pinto, I., Brown, M.T., and Brownlee, C. (2002). Spatiotemporal patterning of reactive oxygen production and Ca²⁺ wave propagation in *Fucus* rhizoid cells. *Plant Cell* **14**: 2369–2381.
- Di Matteo, A., Giovane, A., Raiola, A., Camardella, L., Bonivento, D., De Lorenzo, G., Cervone, F., Bellincampi, D., and Tsernoglou, D. (2005). Structural basis for the interaction between pectin methylesterase and a specific inhibitor protein. *Plant Cell* **17**: 849–858.
- Dutta, R., and Robinson, K.R. (2004). Identification and characterization of stretch-activated ion channels in pollen protoplasts. *Plant Physiol.* **135**: 1398–1406.
- Fasano, J.M., Swanson, S.J., Blancaflor, E.B., Dowd, P.E., Kao, T.H., and Gilroy, S. (2001). Changes in root cap pH are required for the gravity response of the *Arabidopsis* root. *Plant Cell* **13**: 907–921.
- Foreman, J., Demidchik, V., Bothwell, J.H., Mylona, P., Miedema, H., Torres, M.A., Linstead, P., Costa, S., Brownlee, C., Jones, J.D., Davies, J.M., and Dolan, L. (2003). Reactive oxygen species produced by NADPH oxidase regulate plant cell growth. *Nature* **422**: 442–446.
- Frantz, C., Barreiro, G., Dominguez, L., Chen, X.M., Eddy, R., Condeelis, J., Kelly, M.J.S., Jacobson, M.P., and Barber, D.L. (2008). Cofilin is a pH sensor for actin free barbed end formation: Role of phosphoinositide binding. *J. Cell Biol.* **183**: 865–879.
- Galione, A., and Churchill, G.C. (2002). Interactions between calcium release pathways: Multiple messengers and multiple stores. *Cell Calcium* **32**: 343–354.
- Gao, H., Gong, Y.W., and Yuan, Y.J. (2007). RGD-dependent mechanotransduction of suspension cultured *Taxus* cell in response to shear stress. *Biotechnol. Prog.* **23**: 673–679.

- Garcia-Brugger, A., Lamotte, O., Vandelle, E., Bourque, S., Lecourieux, D., Poinssot, B., Wendehenne, D., and Pugin, A. (2006). Early signaling events induced by elicitors of plant defenses. *Mol. Plant Microbe Interact.* **19**: 711–724.
- Gus-Mayer, S., Naton, B., Hahlbrock, K., and Schmelzer, E. (1998). Local mechanical stimulation induces components of the pathogen defense response in parsley. *Proc. Natl. Acad. Sci. USA* **95**: 8398–8403.
- Haley, A., Russell, A.J., Wood, N., Allan, A.C., Knight, M., Campbell, A.K., and Trewavas, A.J. (1995). Effects of mechanical signaling on plant cell cytosolic calcium. *Proc. Natl. Acad. Sci. USA* **92**: 4124–4128.
- Hamant, O., Heisler, M.G., Jonsson, H., Krupinski, P., Uyttewaal, M., Bokov, P., Corson, F., Sahlín, P., Boudaoud, A., Meyerowitz, E.M., Couder, Y., and Traas, J. (2008). Developmental patterning by mechanical signals in *Arabidopsis*. *Science* **322**: 1650–1655.
- Hardham, A.R., Takemoto, D., and White, R.G. (2008). Rapid and dynamic subcellular reorganization following mechanical stimulation of *Arabidopsis* epidermal cells mimics responses to fungal and oomycete attack. *BMC Plant Biol.* **8**: 63.
- Hedrich, R., Busch, H., and Raschke, K. (1990). Ca²⁺ and nucleotide dependent regulation of voltage dependent anion channels in the plasma membrane of guard cells. *EMBO J.* **9**: 3889–3892.
- Jaffe, M.J., Leopold, A.C., and Staples, R.C. (2002). Thigmo responses in plants and fungi. *Am. J. Bot.* **89**: 375–382.
- Kerr, E.M., and Fry, S.C. (2004). Extracellular cross-linking of xylan and xyloglucan in maize cell-suspension cultures: The role of oxidative phenolic coupling. *Planta* **219**: 73–83.
- Kimbrough, J.M., Salinas-Mondragon, R., Boss, W.F., Brown, C.S., and Sederoff, H.W. (2004). The fast and transient transcriptional network of gravity and mechanical stimulation in the *Arabidopsis* root apex. *Plant Physiol.* **136**: 2790–2805.
- Kinoshita, T., Nishimura, M., and Shimazaki, K. (1995). Cytosolic concentration of Ca²⁺ regulates the plasma membrane H⁺-ATPase in guard cells of fava bean. *Plant Cell* **7**: 1333–1342.
- Knight, H. (2000). Calcium signaling during abiotic stress in plants. *Int. Rev. Cytol.* **195**: 269–324.
- Knight, M.R., Campbell, A.K., Smith, S.M., and Trewavas, A.J. (1991). Transgenic plant aequorin reports the effects of touch and cold-shock and elicitors on cytoplasmic calcium. *Nature* **352**: 524–526.
- Kramer, V.L. (2004). A Role for Calmodulin and Actin in the Gravitropism of Plant Roots. Master's thesis (University Park, PA: Penn State University).
- Lapous, D., Mathieu, Y., Guern, J., and Lauriere, C. (1998). Increase of defense gene transcripts by cytoplasmic acidification in tobacco cell suspensions. *Planta* **205**: 452–458.
- Leblanc-Fournier, N., Coutand, C., Crouzet, J., Brunel, N., Lenne, C., Moulia, B., and Julien, J.L. (2008). Jr-ZFP2, encoding a Cys2/His2-type transcription factor, is involved in the early stages of the mechano-perception pathway and specifically expressed in mechanically stimulated tissues in woody plants. *Plant Cell Environ.* **31**: 715–726.
- Lee, D., Polisensky, D.H., and Braam, J. (2005). Genome-wide identification of touch- and darkness-regulated *Arabidopsis* genes: A focus on calmodulin-like and XTH genes. *New Phytol.* **165**: 429–444.
- Legue, V., Blancaflor, E., Wymer, C., Perbal, G., Fantin, D., and Gilroy, S. (1997). Cytoplasmic free Ca²⁺ in *Arabidopsis* roots changes in response to touch but not gravity. *Plant Physiol.* **114**: 789–800.
- Lewis, B.D., and Spalding, E.P. (1998). Nonselective block by La³⁺ of *Arabidopsis* ion channels involved in signal transduction. *J. Membr. Biol.* **162**: 81–90.
- Liedtke, W. (2008). Molecular mechanisms of TRPV4-mediated neural signaling. *Ann. N. Y. Acad. Sci.* **1144**: 42–52.
- Lino, B., Baizabal-Aguirre, V.M., and Gonzalez de la Vara, L.E. (1998). The plasma-membrane H⁺-ATPase from beet root is inhibited by a calcium-dependent phosphorylation. *Planta* **204**: 352–359.
- Massa, G.D., and Gilroy, S. (2003). Touch modulates gravity sensing to regulate the growth of primary roots of *Arabidopsis thaliana*. *Plant J.* **33**: 435–445.
- McAinsh, M.R., and Pittman, J.K. (2009). Shaping the calcium signature. *New Phytol.* **181**: 275–294.
- Meng, S.X., Lieffers, V.J., Reid, D.E.B., Rudnicki, M., Silins, U., and Jin, M. (2006). Reducing stem bending increases the height growth of tall pines. *J. Exp. Bot.* **57**: 3175–3182.
- Messerli, M.A., Danuser, G., and Robinson, K.R. (1999). Pulsatile influxes of H⁺, K⁺ and Ca²⁺ lag growth pulses of *Lilium longiflorum* pollen tubes. *J. Cell Sci.* **112**: 1497–1509.
- Messerli, M.A., and Robinson, K.R. (1998). Cytoplasmic acidification and current influx follow growth pulses of *Lilium longiflorum* pollen tubes. *Plant J.* **16**: 87–91.
- Mitchell, C.A. (1996). Recent advances in plant response to mechanical stress: Theory and application. *HortScience* **31**: 31–35.
- Monshausen, G.B., Bibikova, T.N., Messerli, M.A., Shi, C., and Gilroy, S. (2007). Oscillations in extracellular pH and reactive oxygen species modulate tip growth of *Arabidopsis* root hairs. *Proc. Natl. Acad. Sci. USA* **104**: 20996–21001.
- Monshausen, G.B., and Gilroy, S. (2009). Feeling green: Mechano-sensing in plants. *Trends Cell Biol.* **19**: 228–235.
- Monshausen, G.B., Messerli, M.A., and Gilroy, S. (2008a). Imaging of the Yellow Cameleon 3.6 indicator reveals that elevations in cytosolic Ca²⁺ follow oscillating increases in growth in root hairs of *Arabidopsis*. *Plant Physiol.* **147**: 1690–1698.
- Monshausen, G.B., and Sievers, A. (1998). Weak mechanical stimulation causes hyperpolarisation in root cells of *Lepidium*. *Bot. Acta* **111**: 303–306.
- Monshausen, G.B., Swanson, S.J., and Gilroy, S. (2008b). Touch sensing and thigmotropism. In *Plant Tropisms*, S. Gilroy and P. Masson, eds (Ames, IA, Oxford, UK: Blackwell Publishing), pp. 91–122.
- Mori, I.C., and Schroeder, J.I. (2004). Reactive oxygen species activation of plant Ca²⁺ channels. A signaling mechanism in polar growth, hormone transduction, stress signaling, and hypothetically mechano-transduction. *Plant Physiol.* **135**: 702–708.
- Nagai, T., Yamada, S., Tominaga, T., Ichikawa, M., and Miyawaki, A. (2004). Expanded dynamic range of fluorescent indicators for Ca²⁺ by circularly permuted yellow fluorescent proteins. *Proc. Natl. Acad. Sci. USA* **101**: 10554–10559.
- Ogasawara, Y., et al. (2008). Synergistic activation of the *Arabidopsis* NADPH oxidase AtrbohD by Ca²⁺ and phosphorylation. *J. Biol. Chem.* **283**: 8885–8892.
- Parre, E., and Geitmann, A. (2005). Pectin and the role of the physical properties of the cell wall in pollen tube growth of *Solanum chacoense*. *Planta* **220**: 582–592.
- Price, N.J., Pinheiro, C., Soares, C.M., Ashford, D.A., Ricardo, C.P., and Jackson, P.A. (2003). A biochemical and molecular characterization of LEP1, an extensin peroxidase from lupin. *J. Biol. Chem.* **278**: 41389–41399.
- Regenberg, B., Villalba, J.M., Lanfermeijer, F.C., and Palmgren, M.G. (1995). C-terminal deletion analysis of plant plasma membrane H⁺-ATPase: Yeast as a model system for solute transport across the plant plasma membrane. *Plant Cell* **7**: 1655–1666.
- Sagi, M., and Fluhr, R. (2006). Production of reactive oxygen species by plant NADPH oxidases. *Plant Physiol.* **141**: 336–340.
- Schroeder, J.I., and Hagiwara, S. (1989). Cytosolic calcium regulates

- ion channels in the plasma-membrane of *Vicia faba* guard cells. *Nature* **338**: 427–430.
- Takeda, S., Gapper, C., Kaya, H., Bell, E., Kuchitsu, K., and Dolan, L.** (2008). Local positive feedback regulation determines cell shape in root hair cells. *Science* **319**: 1241–1244.
- Tretner, C., Huth, U., and Hause, B.** (2008). Mechanostimulation of *Medicago truncatula* leads to enhanced levels of jasmonic acid. *J. Exp. Bot.* **59**: 2847–2856.
- Verdoucq, L., Grondin, A., and Maurel, C.** (2008). Structure-function analysis of plant aquaporin AtPIP2;1 gating by divalent cations and protons. *Biochem. J.* **415**: 409–416.
- Walley, J.W., Coughlan, S., Hudson, M.E., Covington, M.F., Kaspi, R., Banu, G., Harmer, S.L., and Dehesh, K.** (2007). Mechanical stress induces biotic and abiotic stress responses via a novel cis-element. *PLoS Genet.* **3**: 1800–1812.
- Yahraus, T., Chandra, S., Legendre, L., and Low, P.S.** (1995). Evidence for a mechanically induced oxidative burst. *Plant Physiol.* **109**: 1259–1266.